

## Supporting Information

### Spectra simulation and kinetic fits

#### 1. Deconvolution of the mass spectra:

In order to evaluate the multiple pathway kinetics in the binding studies we extracted the ratios of the complexes present in solution in a quantitative way.

To achieve this, the mass spectra are simulated with the in-house software *Massign*, as described previously (1-2). The software allows us to extract component spectra for each species present in the mass spectrum. The following steps are taken:

- 1) Peak series (and their masses) are determined by variation of the charge states
- 2) For each species a component spectrum is determined by fitting each peak as a 3 parameter Gaussian, with the peak height chosen according to an envelope function, which mirrors the statistical process of the charge distribution for ESI complexes. Where needed the attachment of buffer / salt water molecules are incorporated for every peak as a trailing slope towards high masses.
- 3) All parameters are optimized so that the sum of all simulated component spectra most closely resembles the experimental spectra
- 4) The integral of each component spectrum can then be used to calculate the percentage of signal originating from a particular complex with respect to all other components.

These percentages can then be used for kinetic analysis, assuming a similar ionization response for all complexes which contain Hsp90 (see paragraph 3).

#### 2. Kinetic model including all pathways:

The kinetic model was set up to include all complexes that were observed using MS. The Hsp90 dimer has two TPR binding sites for either a Hop or a FKBP52, which are both accounted for, while the Hsp90 monomer has one. So for example there are 2 options for an Hsp90 dimer to bind a FKBP52, but only one for the Hsp90 monomer. The whole system is shown **Figure S8**. Since binding of a Hop or FKBP52 to the right or the left binding site of the Hsp90 dimer will be equally likely, we can assume that  $K_{Di} = K_{Di}^*$ . This allows depicting the system in a slightly simpler way, as is used in fig 4 to show our results.

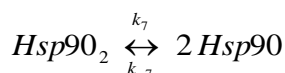
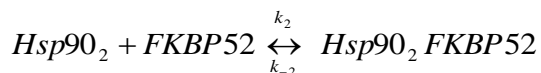
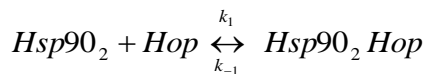
The reactions involved are of the kind:  $A + B \leftrightarrow AB$ , so we use first or second order kinetics for backwards and forward reactions. The  $K_{Di}$ s are determined by the rate constants  $k_i$  as  $K_{Di} = \frac{k_i}{k_{-i}}$

The system of equations which describes the reactions is too complicated to solve directly, so the approach taken here therefore is a numerical one. We input the start concentrations for every component at time point  $t_0$  and then follow the change of concentrations with time step by step. To do that the change in concentration for every component within a small time interval  $dt$  is calculated, taking into account all gains or losses from dissociation or association via all possible pathways. The size of the time interval is not relevant, as long as it

is small enough not to miss a change in the development of the simulated system. The intervals chosen here are  $dt = 0.01$  or  $0.02$  min.

Example:

As shown in **Figure S8** the amount of  $(Hsp90)_2$  is reduced by the formation of the  $(Hsp90)_2$  Hop complex and increases due to the reverse reaction. In addition we have loss and gain from the  $Hsp90_2$  FKBP52 complex and the  $Hsp90$  monomer. To summarize:



The concentration dependence for all three reaction pathways will be according to the equations above. So the concentration ( $c$ ) at time  $t=i+1$  can be determined from the concentrations of all participating components at time  $t=i$ :

$$c(Hsp90_2)_{i+1} = c(Hsp90_2)_i + \left( \begin{aligned} &c(Hsp90_2 Hop)_i \cdot k_1 - c(Hsp90_2)_i \cdot c(Hop)_i \cdot k_{-1} + c(Hsp90_2 FKBP52)_i \cdot k_2 \\ &- c(Hsp90_2)_i \cdot c(FKBP)_i \cdot k_{-2} + c(Hsp90)_i \cdot k_7 - c(Hsp90_2)_i^2 \cdot k_{-7} \end{aligned} \right) dt$$

With the correct rate constants this setup allows us to mimic the development of the concentrations of all components with time. The rate constants are then optimised to minimize the deviation between the simulation and the experimental values. This is calculated from the difference of experimental values to the corresponding theoretical points, using the least square method. In one time course for every time point, all component concentrations are compared to the theoretical counterparts.

The ionization response is similar for all complexes which contain  $Hsp90$ , but not necessarily of the single proteins (see paragraph 3). Therefore those values are part of the simulated system, but are not included in the error function.

### 3. Signal intensity vs. solution concentration.

In order to use the signal intensities for modelling we have to ensure that the ratio of the signal intensities represents the concentration in solution of every component.

Two parameters have to be taken into account:

- 1) The ion detection efficiency of MCP (multi channel plate) detectors
- 2) The ionisation efficiency of the proteins / complexes in the electrospray process.

Figure S9. A shows the % of ions detected by an MCP depending on the ion mass (3). It shows clearly that the ion detection efficiency decreases dramatically with increasing mass. For higher masses the dependency levels off. In our case, all  $Hsp90$ -containing complexes are in a mass range where the variation depending on mass differences is below that of the experimental error. The single proteins (indicated in red) with a smaller mass are not included in the error function for the fit optimization. For a broader application of this modelling method a correction factor could be used to integrate proteins of different mass ranges into the modelling.

To show that the behaviour of the signal intensity is linear in the relevant mass area titration experiments were performed. Figure S9D shows a titration of glutamate dehydrogenase (glut) (336 kDa) with Hsp90. Glutamate dehydrogenase was chosen, since it represents the mass range of the Hsp90 containing complexes in the performed binding studies. Figure S9C shows two spectra of this titration in comparison with a spectrum of complexes formed by Hsp90, Hop and FKBP52. Figure S9D shows the correlation of the signal response of Hsp90 is indeed linear with regard to GD with a slope determined to be  $1.07 \pm 0.07$ .

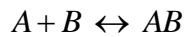
Differences in ionisation efficiency can be detected by monitoring the amount of signal corresponding to every protein (free or bound) during a timecourse. Example : the amount of Hop in a sample is represented by all Hop-containing complexes in the following way for a Hsp90 Hop solution:

$$\Sigma(\text{Hop}) = [\text{Hop}] + [\text{Hsp90}_2 \text{ Hop}] + 2*[\text{Hsp90}_2 \text{ Hop}_2 ]$$

If the ionisation efficiency of free Hop were for example higher than of a Hop-containing complex the formation of Hsp90 Hop complexes (and therefore a decrease of free Hop) would lead to an apparent loss of the overall Hop signal. Figure S9B shows these summed intensities (scaled by overall Hsp90 signal, as explained below in paragraph 5 for the examples of time courses depicted in Fig. 2 and Figure S4. No increase or decrease in overall concentration of the proteins was observed. For a more general application of this method the change in observed overall signal of one protein could be accounted for and corrected.

#### 4. Comparing intensity ratio to concentration of components

The experimentally determined component ratios are extracted from the mass spectra by simulation of the individual component spectra. This gives us the amount of each component as a % with respect to the overall intensity. So the overall peak intensity is always 100%. But the overall concentration in solution varies with time:



To be able to compare experimental and theoretical values, a scaling factor is introduced for every time step in the simulation. For the error calculation, the theoretical concentrations are also expressed in % with respect to the overall concentration.

#### 5. Correcting for errors in experimental determination of the start concentrations.

To follow kinetic reactions of several components the exact knowledge of the initial concentrations of every component is essential. If working with small quantities at low concentrations this is not always easy to ensure due to errors in concentration measurements and sample handling. Comparing concentrations of all components containing Hop, FKBP52 or Hsp90 for an entire time course however can give the necessary correction factors.

Example: theoretical start concentrations: 1mol Hsp90<sub>2</sub> incubated with 1mol Hop

All Hsp90 containing complexes (taking into account that an Hsp90 dimer splits into two monomers) should at all time points add up to 1mol (closed system). Same holds true for Hop:

$$2*[\text{Hsp90}] + [\text{Hsp90}_2] + [\text{Hsp90}_2 \text{ Hop}] + [\text{Hsp90}_2 \text{ Hop}_2] = 1\text{mol} \quad (1)$$

$$[\text{Hop}] + [\text{Hsp90}_2 \text{ Hop}] + 2*[\text{Hsp90}_2 \text{ Hop}_2] = 1\text{mol} \quad (2)$$

[Hsp90<sub>2</sub> Hop] has to be the same in reaction (1) and (2), independent of how it is calculated. The same is valid for [Hsp90<sub>2</sub> Hop<sub>2</sub>].

Evaluation of the experimental data shows, that this doesn't hold true. This means, that the start concentrations are not always exact, and therefore can't be used for fitting the data.

To correct for this we determine the deviation of the Hop/Hsp90 ratio and the FKBP52/Hsp90 ratio, for every experiment for every time point. (see Figure S9) within one time course the correction factor is determined as the mean of the factors for every time point (**Table S2**). The assumption that is used to correct the starting concentration for Hop and FKBP52 in the fit is that Hsp90 has indeed the expected 1 mol concentration. (So even if this is inaccurate, the ratios determined for Hop/Hsp90 and FKBP52/Hsp90 will be correct)

## 6. Calculating K<sub>D</sub>s for binary, ternary and higher systems:

We then established the K<sub>D</sub>s, which determine the complex formation between Hsp90, Hop, FKBP52 and Hsp70. To do this we varied the on and off rates in our simulated experiment in a manner to minimize the deviation of the component percentages of our measurements or series of measurements from the simulated ones.

This is less and less reliable the further away the starting values for the on and off rates are. So we started with the simple system of Hsp90 alone. In solution equilibrium establishes between the monomer and dimer. The established values for the Hsp90 dimerization were then kept fixed for the next set of measurements with two proteins: Hsp90 with FKBP52 and Hsp90 with Hop (for the latter different concentration ratios were measured –Fig 1A). This gave values for the binding of two components, which then could be used for the more complicated experiments where Hop or FKBP52 were added to preformed complexes of the other proteins. The start concentrations of the preformed complexes were calculated with the previously established K<sub>D</sub> values and the “adjusted” protein concentrations, determined as described in the previous paragraph.

In a second step the on and off rates were allowed to vary without constraints using the previously determined values as starting values. The K<sub>D</sub> values were then established as the average of the values determined from the 8 different sets of experiments with the standard deviation giving the error.

We then expanded the system to look at possible pathways for Hsp70 binding (Grey arrows **Figure S8**). For this we used two spectra of Hsp90, Hop, and Hsp70 and Hsp90, Hop, FKBP52 and Hsp70 after the systems had reached equilibrium. An Hsp90 dimer has two TPR binding sites, for FKBP52 or Hop. The complexes formed with Hsp70 suggest that Hsp70 can bind a preformed Hsp90 Hop complex, independent of the state of the other binding site (empty or an FKBP52 bound – if the second binding site is also occupied by a Hop a second Hsp70 can also bind). So it is reasonable to assume that the two binding events can be treated independently of bound Hsp70, and therefore the K<sub>D</sub>s treating these events are the same : K<sub>D4</sub> = K<sub>D12</sub> (binding of a FKBP52 to a (Hsp90)<sub>2</sub> Hop Hsp70<sub>0/1</sub>) and K<sub>D5</sub> = K<sub>D13</sub> (binding of a Hop to a (Hsp90)<sub>2</sub> Hop Hsp70<sub>0/1</sub>). The binding of a Hsp70 from our data was found to be similar and can be assumed to depend solely on the Hop-Hsp90 interface and therefore we can expect K<sub>D9</sub> = K<sub>D10</sub> = K<sub>D11</sub> = K<sub>D14</sub>. For the simulation these 4 K<sub>D</sub>s were allowed to vary independently. This was carried out for the Hsp90, Hop, and Hsp70 as well as the Hsp90, Hop, FKBP52, Hsp70 spectrum and then the average value used as Hsp70 binding K<sub>D</sub>, the standard deviation used as error.

We want to emphasize here that we use kinetic modelling to determine thermodynamic values (K<sub>D</sub>s). Even though the rate constants are varied independently, the values determined are the K<sub>D</sub>s – the ratio of the rate




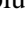

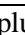



constants. This value mainly determines the equilibrium state of the system. The rate constants, we determine in the process are highly dependent on the exact rise /fall of the concentration curves in the first few minutes and we believe that the accuracy of our measurements in this area might not be sufficient to reliably determine exact rate constants. In general, this might be possible for multicomponent systems which have slower kinetics than in this case.

1. Hernandez H, Makarova OV, EM, Morgner N, Muto Y, Krummel DP, Robinson CV (2009) Isoforms of U1-70k control subunit dynamics in the human spliceosomal U1 snRNP. *PLoS One* 4:e7202.
2. Lane LA, Fernandez-Tornero C, Zhou M, Morgner N, Ptchelkine D, Steuerwald U, Politis A, Lindner D, Gvozdenovic J, Gavin AC, Muller CW, Robinson CV (2011) Mass spectrometry reveals stable modules in holo and apo RNA polymerases I and III. *Structure* 19:90-100.
3. Fraser GW (2002) The ion detection efficiency of microchannel plates (MCPs). *Int J Mass Spectrom* 215:13-30.
4. Mayr C, Richter K, Lilie H, Buchner J (2000) Cpr6 and Cpr7, Two Closely Related Hsp90-associated Immunophilins from *Saccharomyces cerevisiae*, Differ in Their Functional Properties. *J Biol Chem* 275:34140-34146.
5. Wegele H, Haslbeck M, Reinstein J, Buchner J (2003) Sti1 Is a Novel Activator of the Ssa Proteins. *J Biol Chem* 278:25970-25976.
6. Li J, Richter K, Buchner J (2011) Mixed Hsp90-cochaperone complexes are important for the progression of the reaction cycle. *Nat Struct Mol Biol* 18:61-66.
7. Richter K, Muschler P, Hainzl O, Reinstein J, Buchner J (2003) Sti1 is a non-competitive inhibitor of the Hsp90 ATPase - Binding prevents the N-terminal dimerization reaction during the ATPase cycle. *J Biol Chem* 278:10328-10333.
8. Siligardi G, Hu B, Panaretou B, Piper PW, Pearl LH, Prodromou C (2004) Co-chaperone regulation of conformational switching in the Hsp90 ATPase cycle. *J Biol Chem* 279:51989-51998.
9. Prodromou C, Siligardi G, O'Brien R, Woolfson DN, Regan L, Panaretou B, Ladbury JE, Piper PW, Pearl LH (1999) Regulation of Hsp90 ATPase activity by tetratricopeptide repeat (TPR)-domain co-chaperones. *EMBO J* 18:754-762.
10. Pirkl F, Buchner J (2001) Functional analysis of the hsp90-associated human peptidyl prolyl Cis/Trans isomerases FKBP51, FKBP52 and cyp40. *J Mol Biol* 308:795-806.
11. Richter K, Muschler P, Hainzl O, Buchner J (2001) Coordinated ATP Hydrolysis by the Hsp90 Dimer. *J Biol Chem* 276:33689-33696.
12. Hernandez MP, Sullivan WP, Toft DO (2002) The assembly and intermolecular properties of the hsp70-Hop-hsp90 molecular chaperone complex. *J Biol Chem* 277:38294-38304.

### Supporting Tables:

Protein complex	Expected mass (Da)	Measured mass (Da)
(Hsp90) <sub>1</sub>	85443.99	85521 ± 86
(Hsp90) <sub>2</sub>	170887.98	170960 ± 70
FKBP52	52,985	53044 ± 40
Hop	62738.62	62758 ± 44
Hsp70	72231.99	72271 ± 40
(Hsp90) <sub>2</sub> (Hop) <sub>1</sub>	233625	233843 ± 55
(Hsp90) <sub>2</sub> (Hop) <sub>2</sub>	296363	296460 ± 132
(Hsp90) <sub>2</sub> (Hop) <sub>1</sub> (Hsp70) <sub>1</sub>	305856	306400 ± 100
(Hsp90) <sub>1</sub> (FKBP52) <sub>1</sub>	138430	138545 ± 107
(Hsp90) <sub>2</sub> (FKBP52) <sub>1</sub>	223873	223999 ± 52
(Hsp90) <sub>2</sub> (FKBP52) <sub>2</sub>	276858	277015 ± 180
(FKBP52) <sub>1</sub> (Hsp90) <sub>2</sub> (Hop) <sub>1</sub>	286610	286835 ± 140
(FKBP52) <sub>1</sub> (Hsp90) <sub>2</sub> (Hop) <sub>1</sub> (Hsp70) <sub>1</sub>	358841	359441 ± 125
(Hsp90) <sub>2</sub> (Hop) <sub>2</sub> (Hsp70) <sub>1</sub>	368594	369330 ± 61
(Hsp90) <sub>2</sub> (Hop) <sub>2</sub> (Hsp70) <sub>2</sub>	440825	441769 ± 80

**Table S1** Calculated and experimentally measured masses of individual proteins and complexes formed.

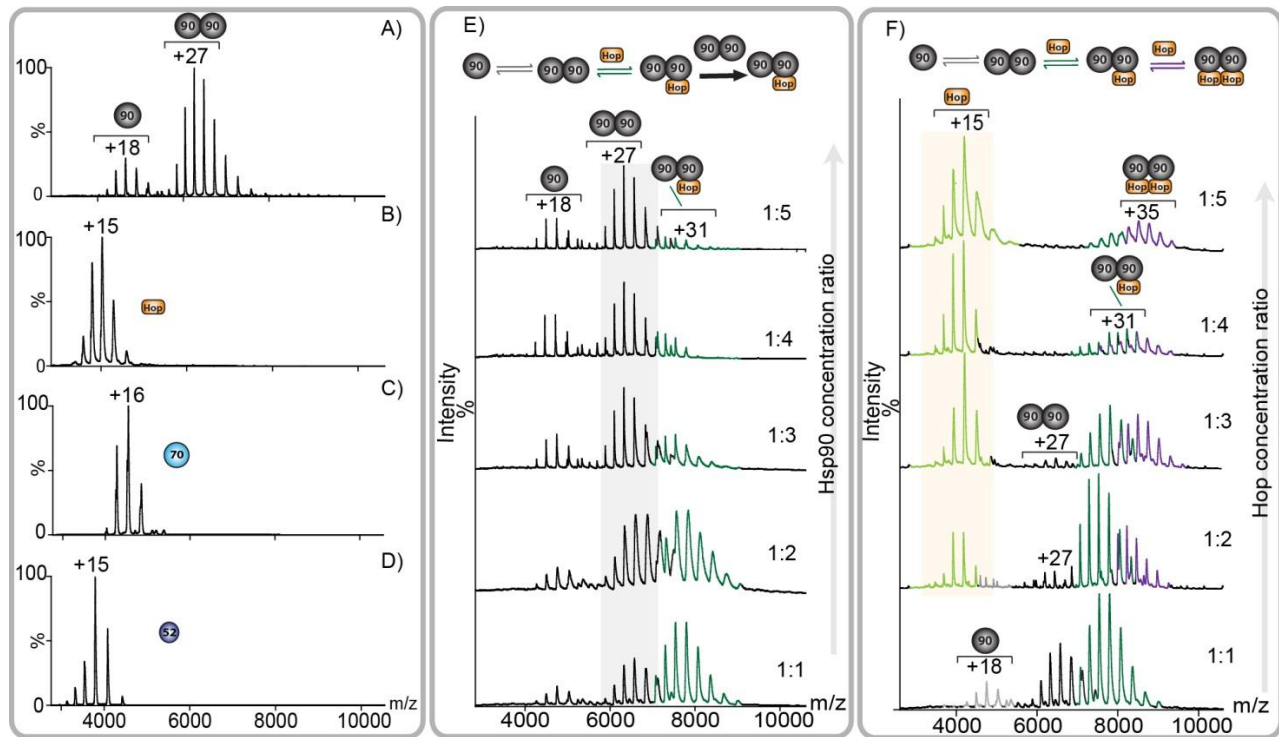
experiment	no. of spectra	concentration correction factor		
		Hop	Fkbp52	Hsp70
(Hsp90) <sub>2</sub> Fkbp52	3		1.13 ± 0.04	
(Hsp90) <sub>2</sub> (Hop) increase Hop	5	0.66 ± 0.07		
(Hsp90) <sub>2</sub> Hop increase Hsp90	5	0.85 ± 0.14		
(Hsp90) <sub>2</sub> Fkbp52 plus Hop	10 	0.84 ± 0.04	1.02 ± 0.05	
	10 	0.61 ± 0.08	0.82 ± 0.04	
	6 	0.82 ± 0.17	1.01 ± 0.09	
(Hsp90) <sub>2</sub> Hop plus Fkbp52	19 	0.60 ± 0.09	0.96 ± 0.03	
	7 	0.62 ± 0.10	0.92 ± 0.03	
	6 	0.74 ± 0.08	1.00 ± 0.06	
(Hsp90) <sub>2</sub> 2hop plus Fkbp52	10 	0.63 ± 0.04	0.75 ± 0.07	
(Hsp90) <sub>2</sub> Hop Hsp70	1 	0.80		0.36
(Hsp90) <sub>2</sub> Hop 70 Fkbp52	1 	0.65	1.03	0.62

**Table S2** Concentration correction factors and number of spectra used for simulations. The coloured symbols are the ones used to represent the  $K_D$  values determined for each dataset in Fig 4.

<b>K<sub>D</sub> value</b>	<b>Complex/stoichiometry</b>	<b>pH</b>	<b>Buffer and salt conditions</b>	<b>Temp °C</b>	<b>concentration</b>
32nM ±8(4)	(yHsp90) <sub>2</sub> -Sti1	7.5	40mM Hepes 20mM KCl	20	80-120nM
22 nM ±7.5(4)	(yHsp90) <sub>2</sub> -Sti1		40mM, 20mM KCL 5mM EDTA		
100nM ±0.02(5)	(yHsp90) <sub>2</sub> -Sti1	7.5	40mM Hepes 150mM KCL 5mM MgCl <sub>2</sub>	25	Up to 30µM
1.5µM ±0.2(5)	Hsp70-Hop				
300nM(5)	(Hsp90:Hop) :Hsp70				
100nM ±0.02(5)	hHsp90-Hop				
53nM(6)	(yHsp90) <sub>2</sub> -(Sti1) <sub>1</sub>	7.5	40mM Hepes 50mM KCL	25	0.01nM – 1µM
<b>ITC</b>					
40nM ±4 (7)	(yHsp90) <sub>2</sub> -Sti1	7.5	40mM Hepes 150mM KCL, 5mM MgCl <sub>2</sub>	25	0-10µM
240nM±70(8)	(yHsp90) <sub>2</sub> -(Sti1) <sub>2</sub>	8	20mM Tris HCL	30	6-90µM
330nM±30(9)	(yHsp90) <sub>2</sub> -(Sti1) <sub>2</sub>	7.4	40mM Tris, 5mM NaCl	30	105 µM Hsp90 :7 µM Sti1 88 µM sti1:5.8 µM Hsp90
55nM ±7(10)	(hHsp90) <sub>2</sub> : (hFkbp52) <sub>2</sub>	8	40mM Hepes	20	320µM Hsp90 monomer: 15µM FKBP52
690nM	(hHsp90) <sub>2</sub> : (Hop) <sub>2</sub>	7.4	50mM Tris, 6mM Mgcl <sub>2</sub> 20mM KCl and 1 mM TECP	25	Up to 3.78mM Hsp90 and 55µM hop
<b>Other methods</b>					
60nM ±12 (11)	WT yHsp90 dimerization	7.5	40 mM HEPES, 150 mM KCl.	20	2nM-1µM
250nM(12)	(Hsp90) <sub>2</sub> :Hsp70:Hop	7.5	10mM Tris-Hcl, 50mM KCl,	30	0.03µM-1.8µM
90nM(12)	(Hsp90) <sub>2</sub> :(Hop) <sub>2</sub>		5mM MgCl 2mM DTT		
1.3uM(12)	Hsp70:Hop				

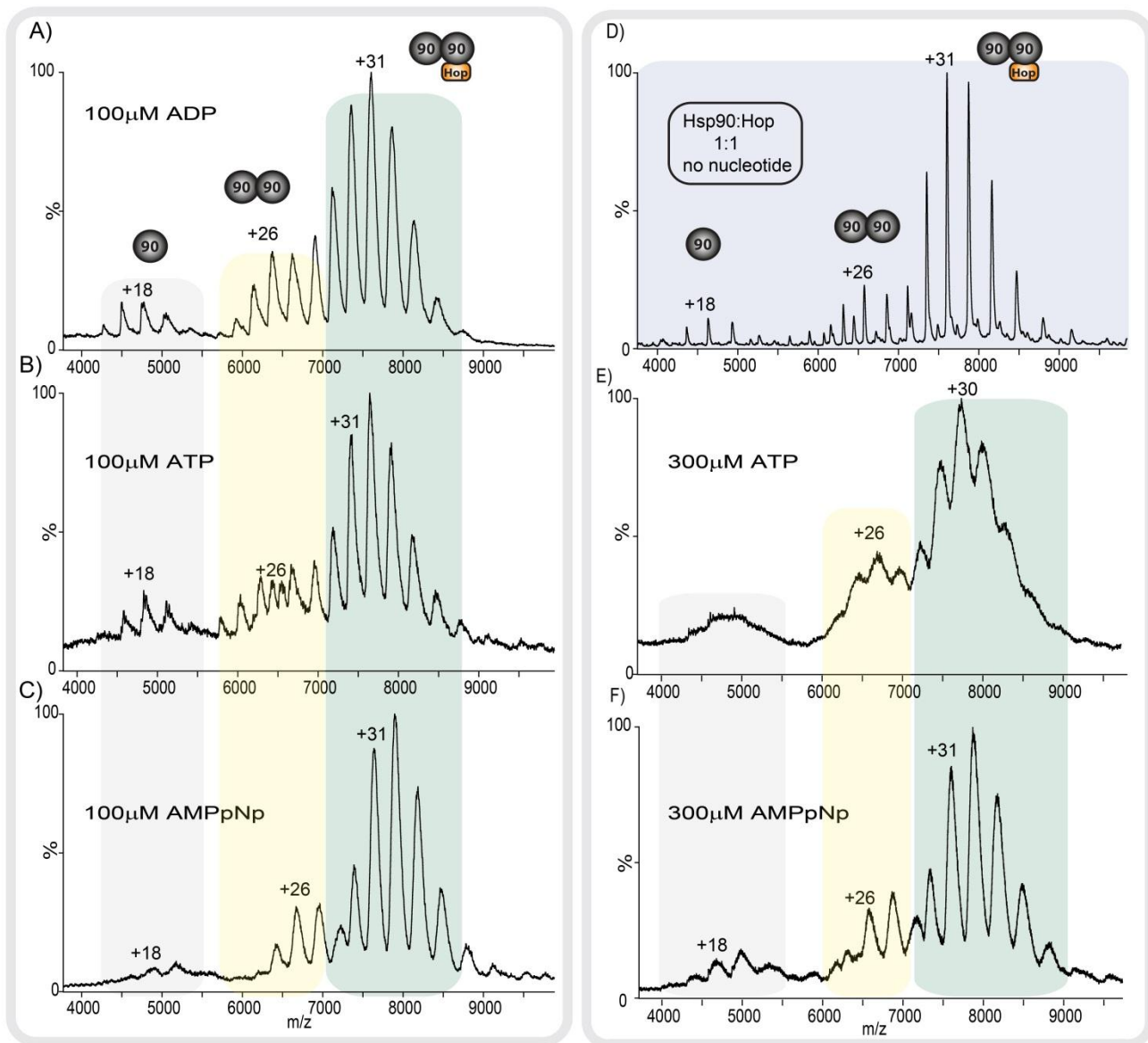
**Table S3** Literature values for yeast (y) and human (h) Hsp90 complexes (graphically represented in **Figure S10**).

## Supporting Figures

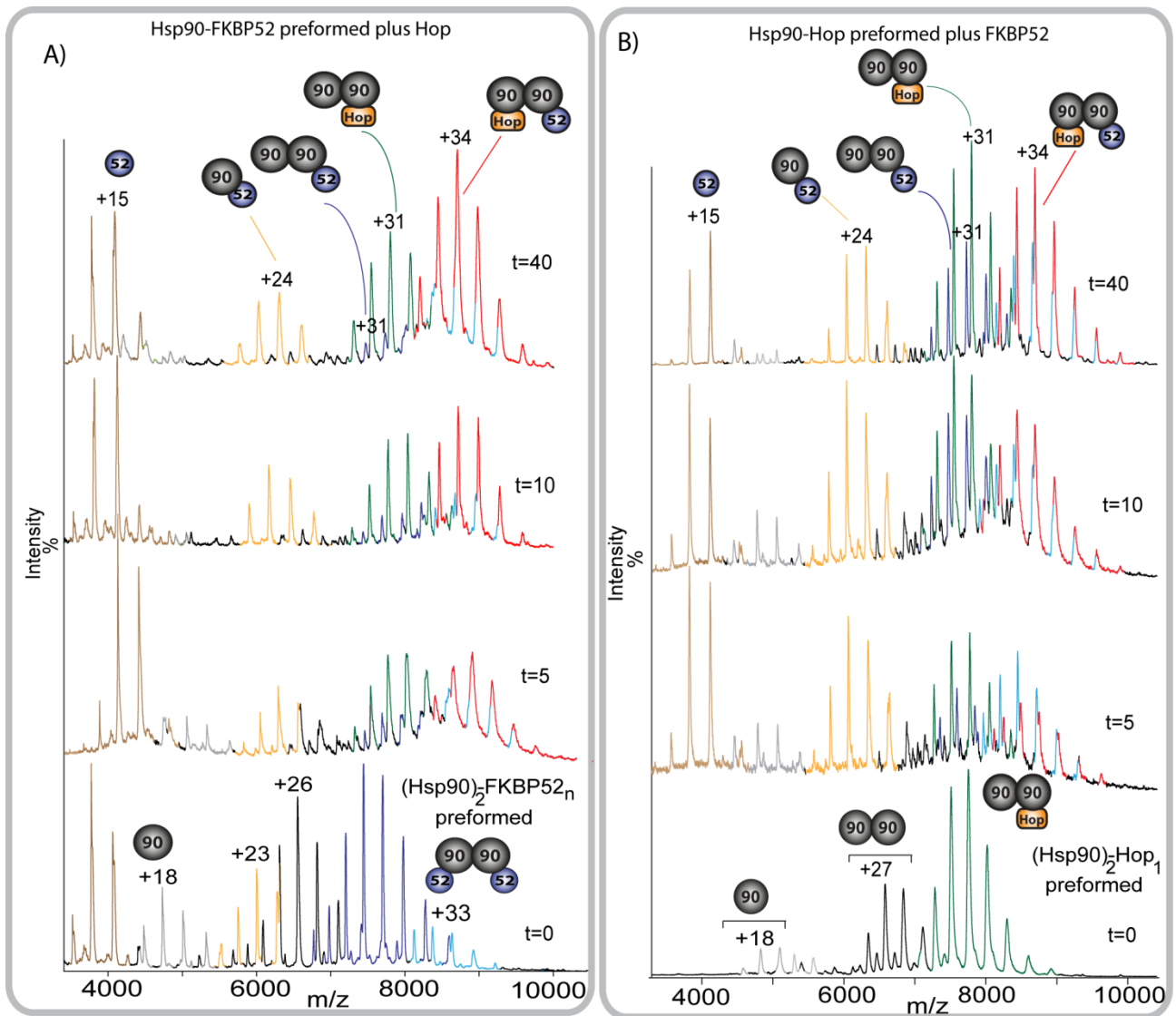


**Figure S1** Mass Spectra of the individual proteins. (A) Mass spectrum of Hsp90 reveals both monomer and predominant dimeric forms. All other proteins used in this study were monomeric. (B) Mass spectrum of Hop. (C) Mass spectrum of Hsp70. Hsp70 shows peak splitting due to truncation of the first 9 N-terminal residues of the His-tag. (D) Mass spectrum of FKBP52. (E) Mass spectra of 1  $\mu$ M Hop incubated with increasing (Hsp90)<sub>2</sub> concentrations. (F) Mass spectra of 1  $\mu$ M (Hsp90)<sub>2</sub> incubated with increasing concentrations of Hop (1  $\mu$ M to 5  $\mu$ M). For (Hsp90)<sub>1</sub> and (Hsp90)<sub>2</sub>, peaks are coloured grey and black respectively. For the (Hsp90)<sub>2</sub>(Hop)<sub>1</sub> and complex (Hsp90)<sub>2</sub>(Hop)<sub>2</sub> complexes, peaks are coloured dark green and purple

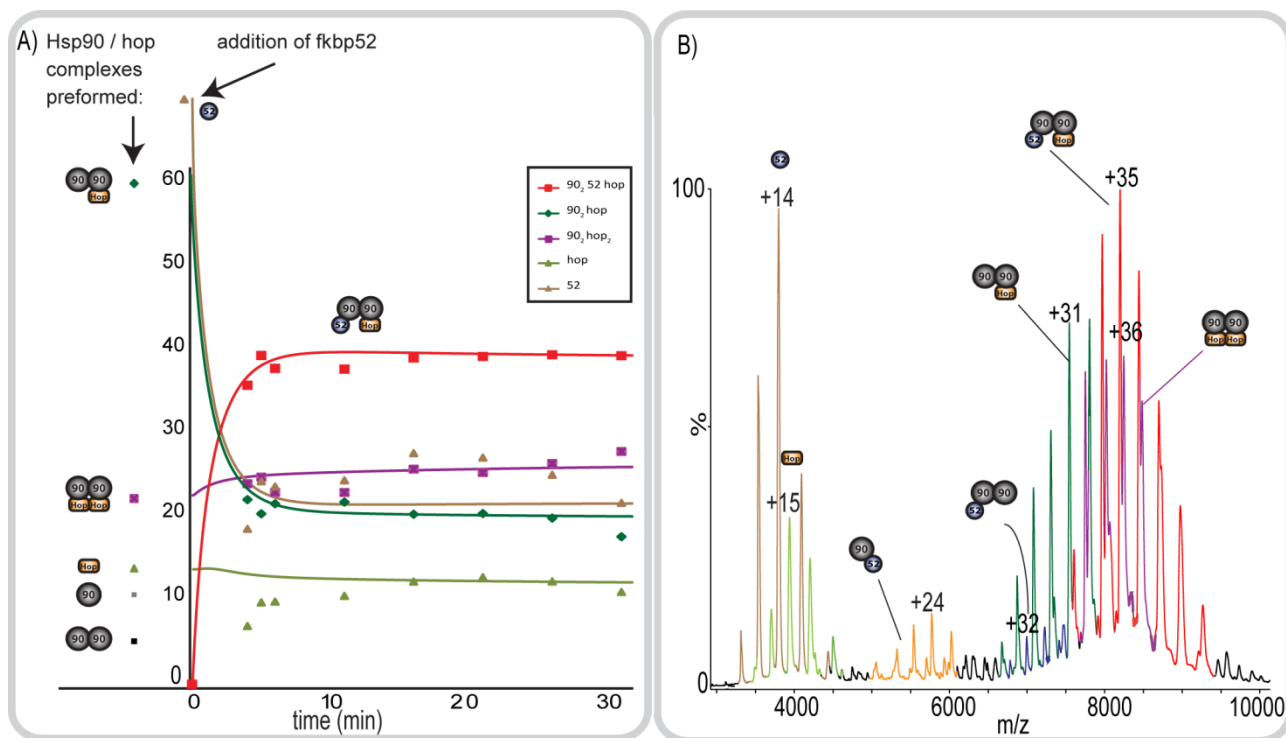




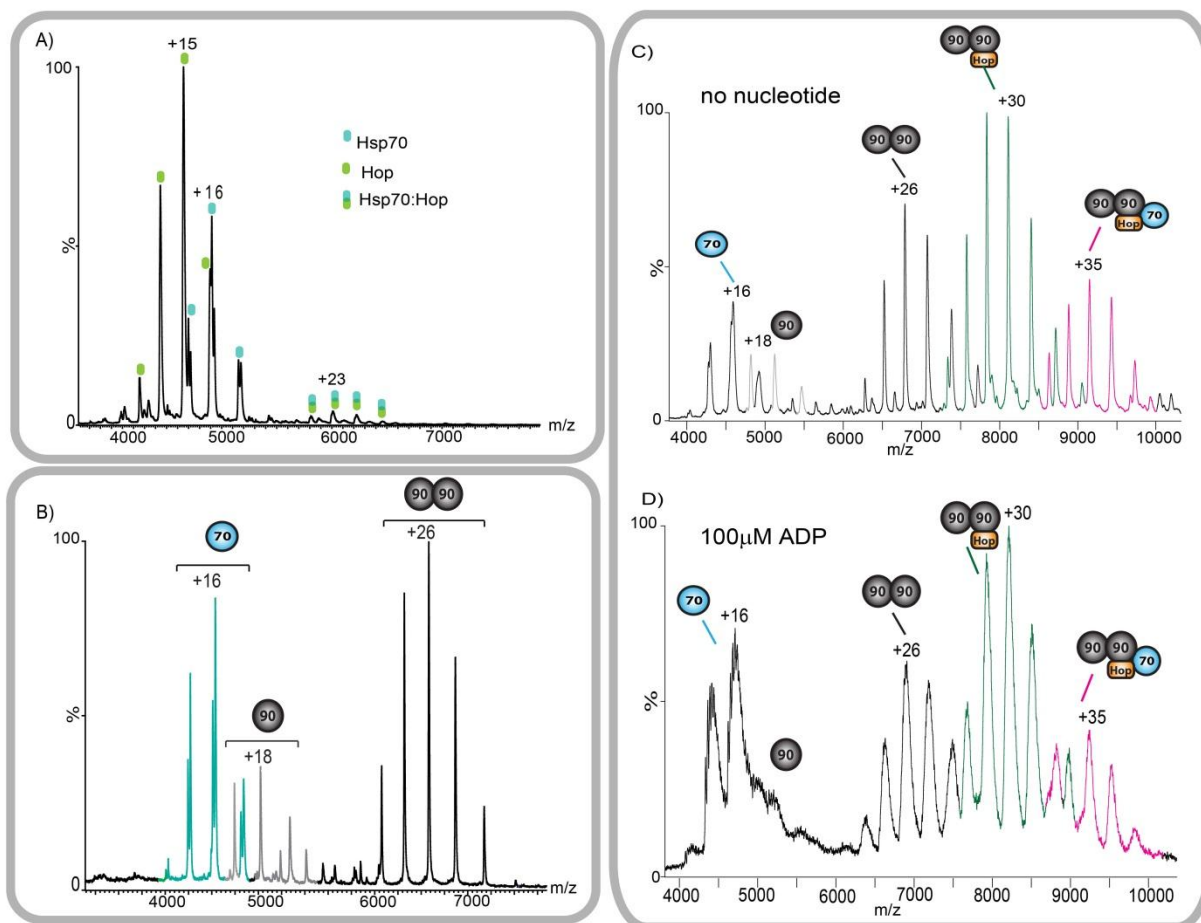
**Figure S2** Effect of nucleotides to an equimolar mixture of  $(\text{Hsp90})_2$  and Hop (both  $1 \mu\text{M}$ ). Addition of  $100 \mu\text{M}$  ADP (A), ATP (B) and AMP-PNP (C) leads to peak broadening, but no effect was observed on the ratios of peaks assigned to the different complexes or complex stoichiometry, if compared to a spectrum taken without any nucleotides added (D). Increase to  $300 \mu\text{M}$  for the nucleotides with a  $K_D$  above  $100 \mu\text{M}$ : ATP (E) and AMP-PNP (F) shows the same results.



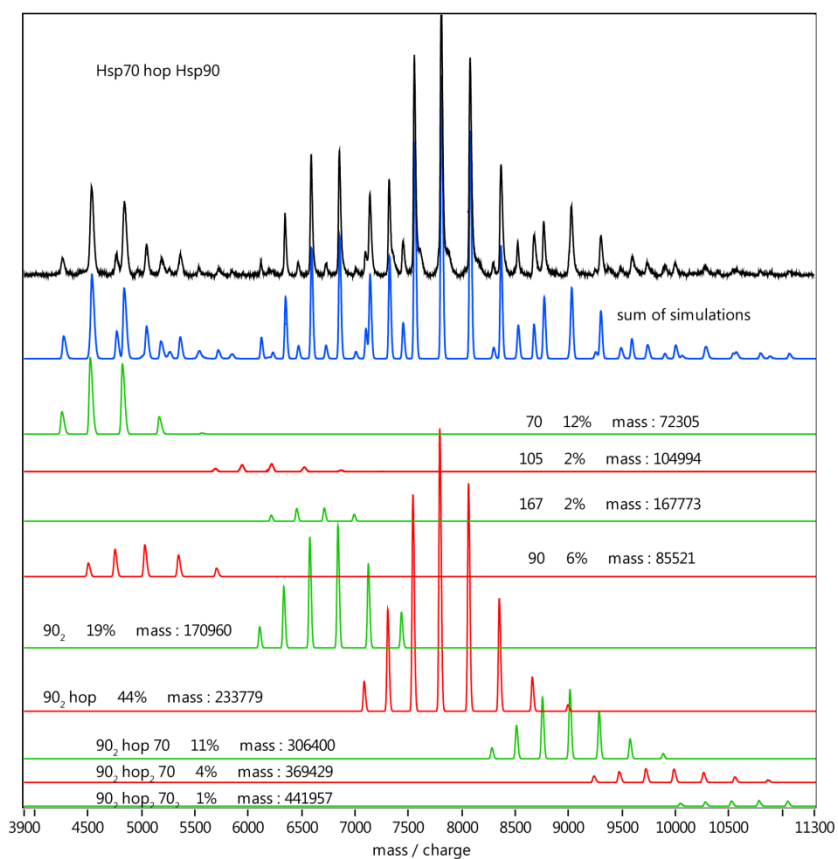
**Figure S3 Formation of asymmetric complexes between Hop, FKBP52 and Hsp90.** A) Bottom panel shows complexes of Hsp90 and FKBP52, preformed at equimolar concentration (1  $\mu\text{M}$ ). Hop is added (1  $\mu\text{M}$ ) and mass spectra recorded at different time points. B) MS spectrum recorded for  $(\text{Hsp90})_2$  Hop complexes preformed at equimolar concentration with FKBP52 added subsequently at an equimolar ratio. The unbound Hsp90 dimer is represented by the black peaks. Complexes formed are colour coded for  $(\text{Hsp90})_1(\text{FKBP52})_1$  orange,  $(\text{Hsp90})_2(\text{Hop})_1$  (dark green),  $(\text{Hsp90})_2(\text{FKBP52})_1$  (dark blue),  $(\text{Hsp90})_2(\text{FKBP52})_2$  (light blue) and  $(\text{Hsp90})_2(\text{Hop})_1(\text{FKBP52})_1$  (red).



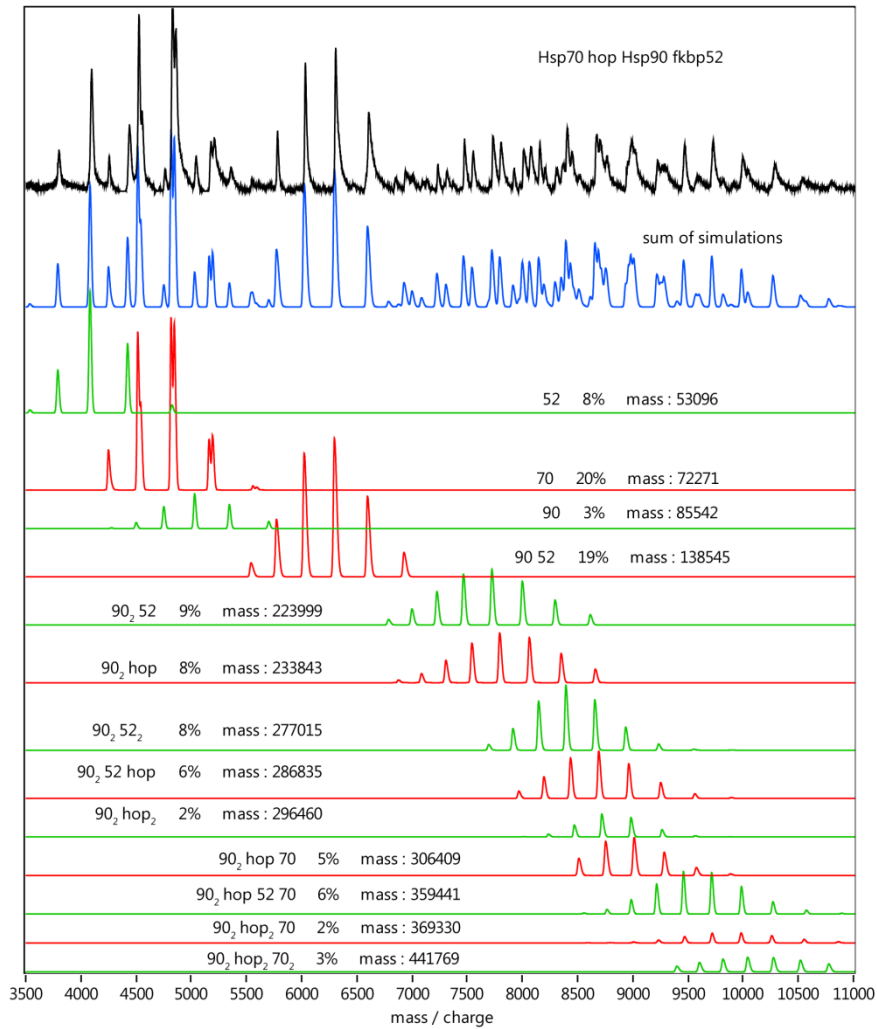
**Figure S4** A) Complexes of Hsp90 and Hop are preformed and then FKBP52 is added. Binding behaviour of FKBP52 to  $(Hsp90)_2 : Hop_n$   $n = 1$  or  $2$  is monitored. The formation of ternary  $(Hsp90)_2 : Hop : FKBP52$  happens via binding of FKBP52 to the free binding site of  $(Hsp90)_2 : Hop_1$  leaving the  $(Hsp90)_2 : Hop_2$  population unaltered.  $(Hsp90)_m : FKBP52_n$  form as well with  $n, m = 1$  or  $2$ , with  $n \leq m$ . For simplicity after  $t=0$  only the development of the Hop containing complexes is shown here. B) Mass spectrum recorded after 3 h for system described in A). The asymmetric complex is the major species. Peaks observed represent unbound Hop (light green),  $(Hsp90)_2(Hop)_1$  (dark green),  $(Hsp90)_2(Hop)_2$  (purple) and with very low intensity Hsp90 monomer and dimer (grey and black respectively). The  $(Hsp90)_1(FKBP52)_1$  and  $(Hsp90)_2(FKBP52)_1$  complexes are coloured yellow and blue respectively and the  $(Hsp90)_2(Hop)_1(FKBP52)_1$  complex shown in red.



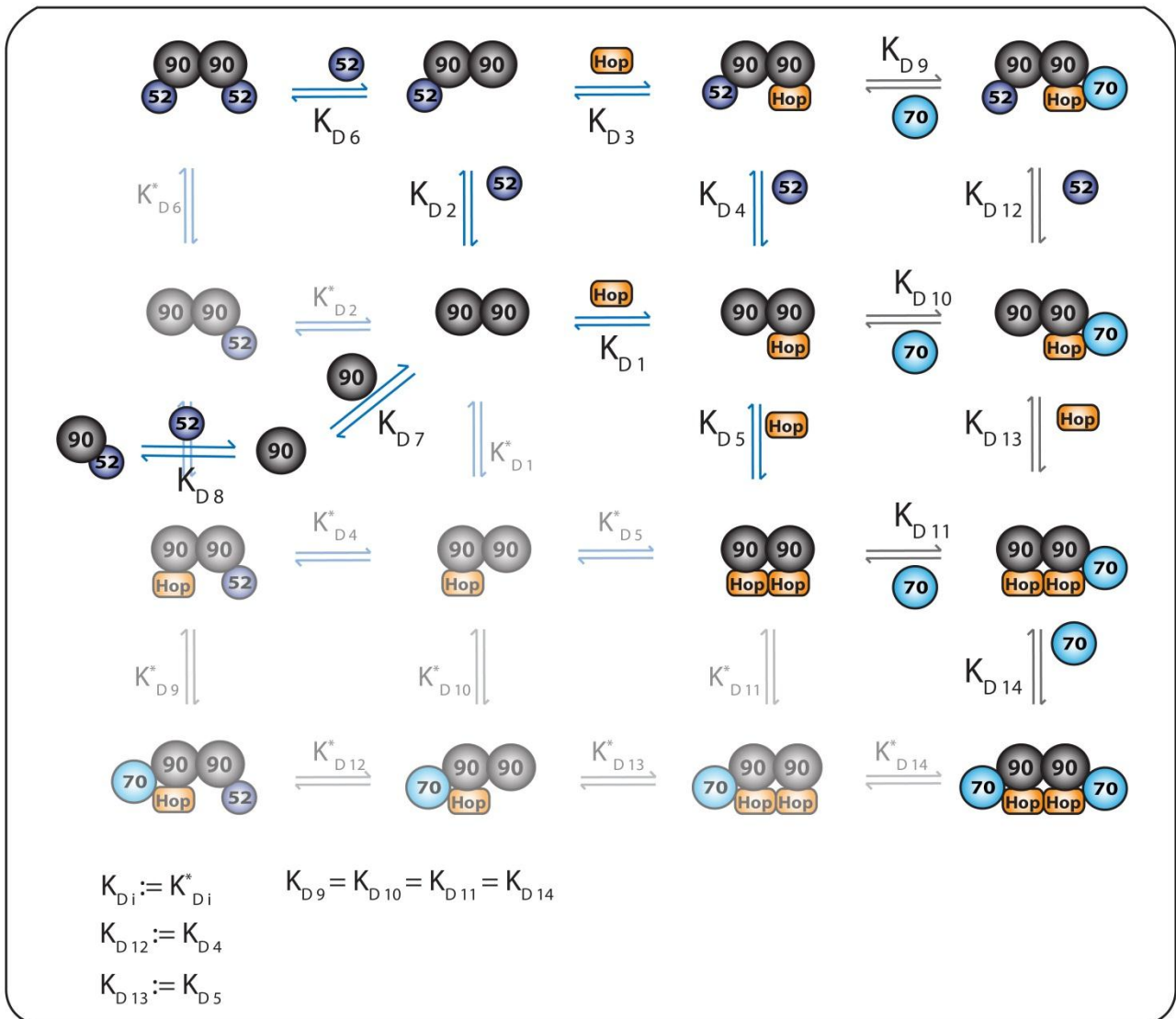
**Figure S5** A) MS spectrum recorded for 2  $\mu\text{M}$  Hop with 1  $\mu\text{M}$  Hsp70 showing weak binding in the presence of 100  $\mu\text{M}$  ADP. B) MS spectrum recorded for Hsp90 and Hsp70 showing no binding. C) MS spectrum of the intermediate complex  $(\text{Hsp90})_2(\text{Hop})_1(\text{Hsp70})_1$  without nucleotides and D) in the presence of 100  $\mu\text{M}$  ADP. Peaks correspond to unbound Hsp70 (green), Hsp90 monomer and dimer (grey and black respectively). The Hsp90 dimer and Hop monomer complex (dark green) and the intermediate complex (pink). Addition of ADP leads to peak broadening but no change in the ratios of the peaks from different complexes or complex stoichiometry.



**Figure S6** Spectral deconvolution of the Hsp70:Hop:Hsp90 complexes. The experimental spectra (black) and the sum of all simulations (blue) are shown. The individually simulated charge state distributions are shown in red and green, their masses, identities and percentages are stated. The mass series 105kDa and 167kDa are not identified as they are likely contaminants



**Figure S7** Spectral deconvolution of the intermediate complex plus FKBP52. The experimental spectra (black) and the sum of all simulations (blue) are shown. The individually simulated charge state distributions (red and green) and their masses, identities and percentages are stated.



**Figure S8** Model system used to determine  $K_{D,S}$ , set up to include all experimentally observed proteins and complexes. The two binding sites of Hsp90 dimer were treated separately, but the evolving on and off rates of the analogue complexes (e.g. Hop binding the right or the left  $(\text{Hsp90})_2$  binding site) were set to be equal (therefore  $K_{D_i} = K_{D_i}^*$ ). This allows collapsing the whole system (opaque and transparent) to the opaque one, which is used to illustrate our results (Fig 4). The  $K_{D,S}$  which were set to be equal or determined to be equal are indicated.

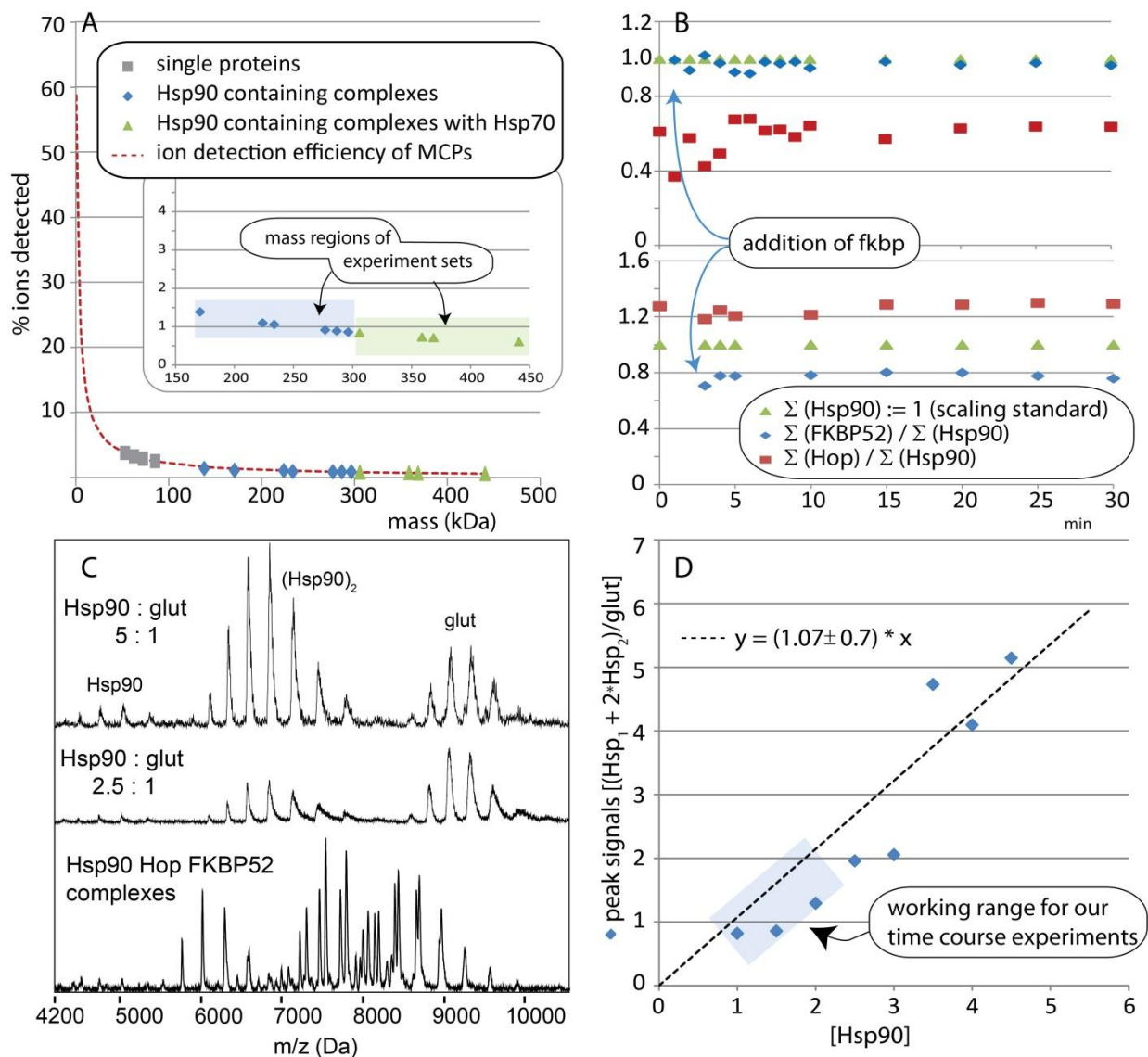


Figure S9 A) Ion detection efficiency for MCPs decreases rapidly for small masses, but levels off for higher mass ions. The mass regions used in this study are indicated in the insert (blue Hsp90-containing complexes and green Hsp90- Hsp70-containing complexes). The detector response for complexes is within the range  $1 \pm 0.25$ . Since this value is very small and made very little difference to our calculation (<10% of the experimental error) we did not consider it further. B) Plot of the overall intensity of the proteins (free and bound) against time (mins) over the period of complex formation (time courses shown in in Fig. 2 and Figure S4). Since this is a closed system the amount of a particular protein should remain constant throughout. If proteins when incorporated into the different complexes are ionized with greater or lower efficiency, changes in intensity would occur. In our case the observed signals remain essentially constant



and no difference between ionization efficiency of free or bound proteins could be detected. C)

Representative mass spectra of the complexes investigated in this study (bottom) compared with spectra of Hsp90 at different concentrations and glutamate dehydrogenase as internal standard, used for the titration curve(D) in which the sum of the signals assigned to Hsp90 are divided by those of glutamine dehydrogenase and plotted against the concentration of Hsp90. .

literature values of Published  $K_D$  values compared to those measured in this study

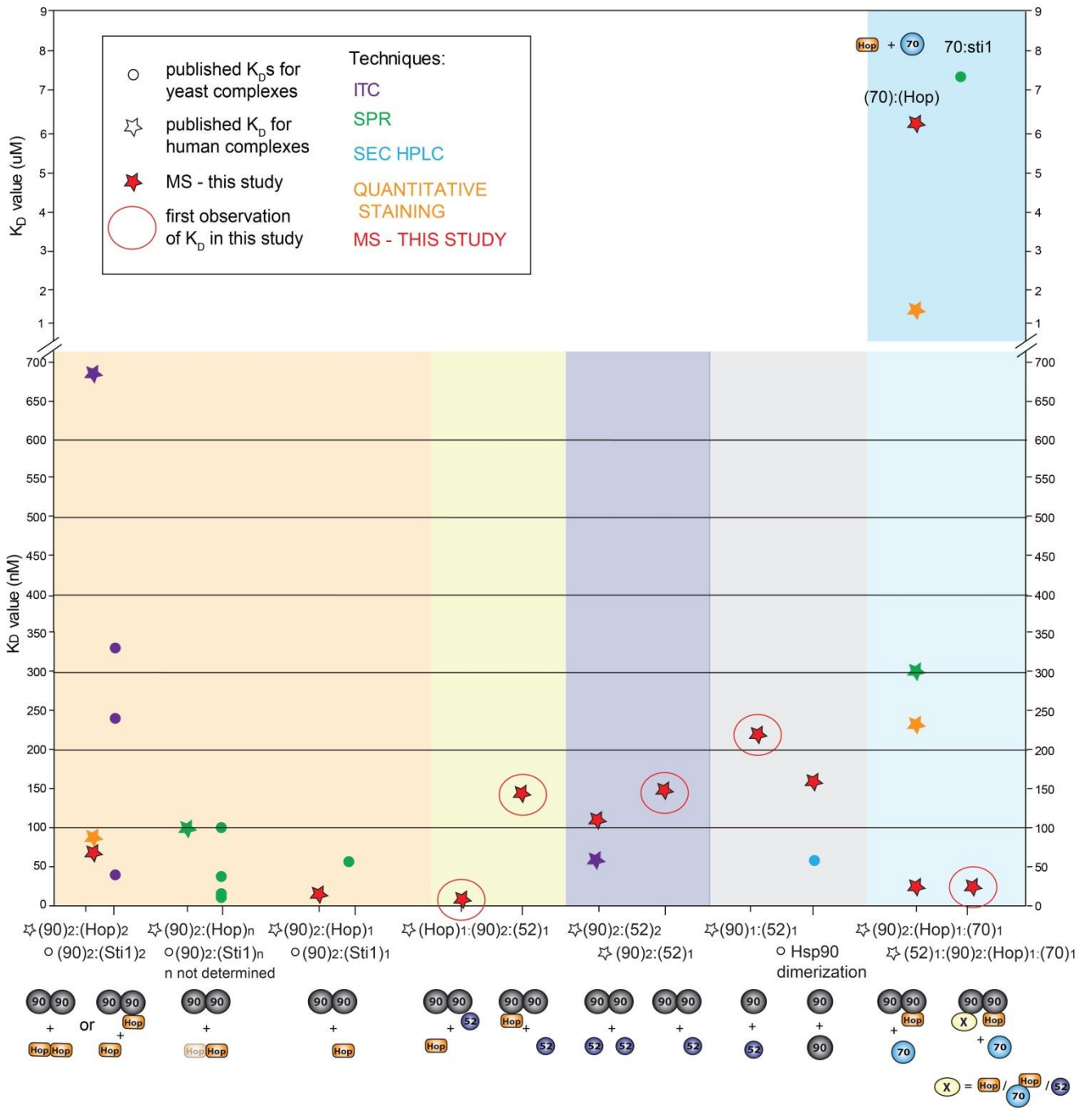


Figure S10 literature values of published  $K_D$ s compared to those measured in this study